IEEE Access
Multidisciplinary ⋮ Rapid Review ⋮ Open Access Journal

Received 17 November 2023, accepted 19 December 2023, date of publication 22 December 2023,
date of current version 16 January 2024.

Digital Object Identifier 10.1109/ACCESS.2023.3346037

RESEARCH ARTICLE

Maximizing Output Power Using a Magnetic Energy Harvesting System Considering the Relationship Between Harvesting Time and Induced Voltage Due to a Change of Airgap

SUNGRYUL HUH[1], (Graduate Student Member, IEEE), JA-IL KOO[2], OKHYUN JEONG[3], (Member, IEEE), AND SEUNGYOUNG AHN[1], (Senior Member, IEEE)

[1]Cho Chun Shik Graduate School of Mobility, Korea Advanced Institute of Science and Technology, Daejeon 34051, South Korea
[2]Ferraris Power Inc., Las Vegas, NV 89119, USA
[3]Department of Electronic Engineering, Sogang University, Seoul 04107, South Korea

Corresponding author: Seungyoung Ahn (sahn@kaist.ac.kr)

This work was supported by the Institute of Information & Communications Technology Planning & Evaluation (IITP) funded by the Korean Government (MSIT) through the Development of 3.3 kW Cluster Wireless Charging Technologies for Robot under Grant 2022-0-00452.

ABSTRACT Power transmission lines are equipped with various electronic devices, including power line inspection robots, safety sensors, and monitoring systems. However, providing power to devices installed on these lines often requires extensive construction and poses many challenges. Therefore, to solve such problems, active research is being conducted on Magnetic Energy Harvesters (MEHs) that harness the magnetic field generated by the current in the power lines to harvest electricity. A crucial design objective of the MEH is to maximize harvested power even if the saturated region is partially included, unlike a current transformer (CT), which must maintain an unsaturated state throughout the operating region. In this paper, design considerations of an MEH are discussed in comparison to the CT. Specifically, this paper formulates the relationship of the airgap between core cutting surfaces, the timing of power harvesting, and the amount of harvested power. It was observed that the MEH core should be designed to have a B-H curve close to the step function by minimizing the airgap and selecting magnetic material with high saturation magnetic flux density to achieve high harvesting power. An optimal MEH model for harvesting the maximum power for each given input current condition is presented. Furthermore, experiments were conducted to verify that 28 W of power was harvested under the input current condition of 150 Arms.

INDEX TERMS Energy harvesting, magnetic material, magnetic saturation, magnetic core.

I. INTRODUCTION

Electric energy is supplied through power lines which span millions of kilometers in length and are exposed to the external environment. These power lines can be damaged by natural hazards such as lightning, wildfires, and fallen trees. To ensure the reliable operation of electrical power systems, constant monitoring and preventive maintenance work are necessary. Recently, as depicted in Fig. 1, the environment surrounding power lines has been monitored using numerous sensors, cameras, and drones, as in [1], [2], and [3]. In addition, various robots are being employed to repair malfunctions. This approach has the potential to reduce maintenance costs and minimize human exposure to hazardous environments. However, many devices in the industry depend on battery power, which has a limited capacity. This reliance on batteries leads to inconveniences such as periodic battery replacements and high maintenance costs. To address these limitations, energy harvesting (EH) technologies by solar, wind, and magnetic fields, have emerged as an appealing solution to enable self-sustainability in systems, eliminating the need for battery power.

The associate editor coordinating the review of this manuscript and approving it for publication was Francesco G. Della Corte.

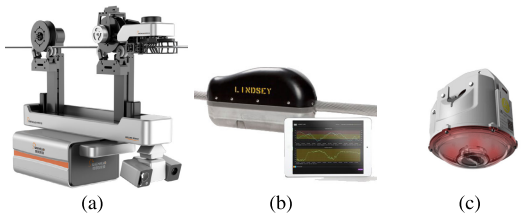

FIGURE 1. Various equipment for transmission line maintenance: (a) Transmission Line Inspection Robot by SHENHAO [1], (b) Transmission Line Conductor Monitor by LINDSEY [2], and (c) Overhead Line Sensor by InHand [3]. These devices all require tens of W, or in some cases, even hundreds of W of power. Fundamentally, these devices are powered by batteries, but if they receive power from the power lines through an MEH system, they can be used semi-permanently without needing to replace the batteries.

Energy harvesting is crucial for developing more sustainable, efficient, and innovative energy solutions, which are integral to addressing both present and future energy challenges. Accordingly, research on energy harvesting is being conducted on various topics, such as various sources and various operation methods, as in [4], [5], [6], and [7].

Among the various energy harvesting technologies, magnetic energy harvesters (MEHs) utilize the principle of electromagnetic induction to convert magnetic field energy into usable electrical energy. MEHs typically consist of a coil wound around a magnetic core. When exposed to a varying magnetic field by an alternating current, the magnetic flux through the coil changes, inducing an electromotive force and generating electrical power. MEH systems are able to harvest power with high reliability and high power density in comparison with other energy harvesting sources, as explained in [8], [9], [10], [11], and [12].

The principle of harvesting power through an MEH system is briefly illustrated in Fig. 2(a). Voltage is induced in the core by a magnetic field generated by an alternating current, causing the current to flow, similar to the principle of a wireless power transfer system, as shown in [13] and [14]. This power is then charged to the battery through a rectifier and DC-DC converter. This principle is nearly identical to a current transformer (CT) used to measure current in power lines, and the external appearance is also very similar to that shown in Fig. 2(b) and (c). A CT also uses a core to measure the voltage across a shunt resistor connected to the secondary side and calculates the current on the primary side. CTs are widely used in many applications and have been the subject of extensive research. Accordingly, many research institutions and companies are designing MEH cores based on the design principles of CT cores.

When designing a CT, the most important thing is to design the core so as not to saturate under the current condition in which the CT operates. When the core is saturated, voltage is not induced on the secondary side because the magnetic field does not change with time and has a constant magnitude. Therefore, the current on the primary side cannot be measured on the CT side, and power cannot be harvested in the MEH. Studies [15], [16], [17] suggest that it is important to design the core so that the B-H curve, which expresses the saturation

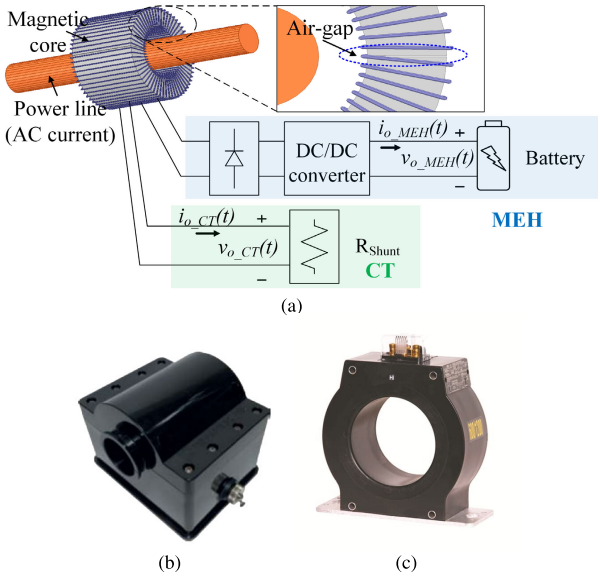

FIGURE 2. Comparison of MEH and CT. (a) Schematics of the MEH and the CT installed on a power line. (b) Magnetic energy harvester by Ferraris Power, Inc. (c) Current transformer by ABB. The appearance and operating principles of MEH and CT are very similar. However, while accuracy is the most critical factor for CTs, the amount of power harvested is the key factor for MEHs. Therefore, these two devices should be designed with different design considerations in mind.

characteristics of the magnetic material, is in the linear region in the operating current range. Previous studies have designed the core to have a linear region in a wide current range by adding an airgap to the core before analyzing the amount of power that can be harvested. These studies introduce an intuitive and simple CT-based design.

However, since an MEH and CT have different purposes, the design method should also differ to obtain the optimal target value for each. The purpose of a CT is to accurately measure the primary side current value; therefore, it must not be saturated in all sections to have high measurement reliability. By adding an airgap to the magnetic core, the linear range of the B-H curve can be expanded, and the saturation current range is increased, as explained in [18] and [19]. Piotr Dworakowski stated that adding an airgap between the cores is designed to have a relatively large size to reduce the slope of the B-H curve and minimize the effect of magnetic saturation on magnetizing inductance in [19]. Particularly, it conducted an analysis of the nonlinear relationship between the number and length of airgaps and effective permeability in three-phase transformers with a multiple airgap structure.

However, the primary purpose of an MEH is to charge the device's battery. It is better to harvest higher power for the same current even if the saturation region is included. To achieve that, instead of reducing the slope of the B-H curve, it is necessary to have as steep a slope as possible to induce a large voltage on the secondary side through a significant change in magnetic flux density under the same operating conditions. Moon suggested that the core should be designed to include a saturation region to maximize

harvesting power in [20]. The harvesting power according to the saturation environment of the core was analyzed mathematically in [20]. Furthermore, in [10], Liu analyzed an MEH system in the saturation region according to the input current condition and proposed a model that could accurately calculate harvesting power by calculating the phase difference by magnetizing inductance.

The harvesting time ($t_{harvest}$) for power generation in the saturation region is not constant and is calculated based on a complex relationship with the design variables of the core and circuit parameters. Additionally, to harvest a significant amount of power, a large magnetic flux density is required relative to the same current conditions, which also varies depending on the design variables of the core. However, previous papers have not analyzed the relationship between the effective B-H curve variation due to design variables of the core, such as the airgap and secondary turns and the maximum magnetic flux density and harvesting time under operating current conditions. The maximum magnetic flux density and harvesting time have a trade-off relationship, and their optimal points vary depending on the surrounding circuit configuration, operating current conditions, and core design methods.

Moreover, not only sensors requiring mW-level low power, but also cameras, robots, and other devices requiring several W or tens of W of power are being installed on power lines. To provide sufficient power to such equipment, at least several W of power must be harvested. However, existing research has only been able to harvest mW-level power using an MEH, and [21] reported a maximum power harvest of 14.3 W under 70 Arms conditions. As the power consumption of devices increases, the current flowing through power lines is also increasing, along with the required power for devices installed on power lines. Consequently, finding new methods to harvest more power at the same current condition is crucial, as well as designing an MEH system that can operate at higher current conditions.

Therefore, this paper proposes an optimal MEH system design method according to the input current condition. First, the differences between CT design and MEH design according to each purpose were analyzed to determine how they should be designed differently. Next, the characteristics of the B-H curve suitable for the MEH core were analyzed, and a core design parameter selection method is presented. In particular, the relationship between the harvesting time due to core saturation and the airgap between the core cut surfaces, which was not considered in previous papers, is formally proposed. Through this, the effect of the airgap of the core on the harvested power can be mathematically derived. Based on the mathematical analysis, many variables were varied and simulated to present an optimal core design according to the input current condition, which was verified through experiments. To validate our proposed design, we conducted experiments using the proposed core design and successfully harvested 28 W of power under the condition of 150 Arms.

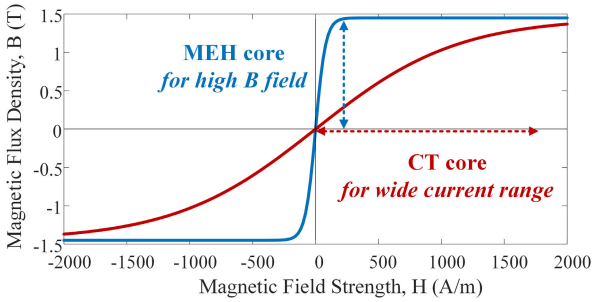

FIGURE 3. MEH and CT's B-H curves for optimal performance. For MEH, a large slope and high saturation flux density are necessary to harvest significant power, while for CT, a BH curve with a low slope allows a wider operating range, thereby increasing measurement accuracy.

This paper is organized as follows. Section II discusses the basic operating principle of an MEH and how it differs from a CT. In Section III, changes in the effective characteristics of the core are confirmed based on changes in various design parameters, and a design method to extract maximum power is analyzed in a given situation. In Section IV, various cores are analyzed through the finite element method (FEM) and circuit simulation, and a model capable of harvesting maximum power under given input current conditions is derived. Section V describes the process and results of the experiments to verify the proposed core designs, and Section VI concludes the paper.

II. COMPARISON OF CURRENT TRANSFORMER AND MAGNETIC ENERGY HARVESTER

Before discussing the optimal MEH design, we must first understand the differences between CTs and MEHs as well as the reasons why designing an MEH core based on the core design consideration of a CT is not recommended. The CT and MEH, which are installed where alternating current flows, such as transmission lines, have similar operating principles and core shapes.

However, the two devices have different objective functions; therefore, they should be designed by different procedures. First, since the purpose of a CT is to measure the current of the power line accurately, it must have high reliability in all areas. Thus, the core should not be saturated within the operating current range of the CT, and the B-H curve of the core should have a wide linear region, as shown in Fig. 3. Additionally, it should allow continuous current flow on the secondary side.

Conversely, as the MEH is a kind of power supply, its purpose is to harvest as much power as possible, necessitating a different design. If the core reaches the saturated region, it cannot harvest power. However, using a core with a small slope B-H curve like the CT core, indicated with a red line in Fig. 3, would result in a very low magnitude of harvested power because it would have a very low magnetic flux density under the operating current condition. Even if saturation occurs within a certain range, using a core with a steep B-H curve, shown as the blue line in Fig. 3, allows for discontinuous but higher average power harvesting.

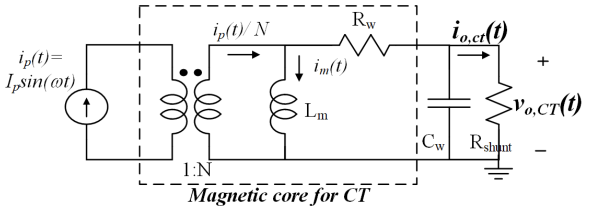

FIGURE 4. Equivalent circuit of CT for measuring primary side current. A resistance, R_{shunt}, is connected for the purpose of converting current to voltage, and the power transmitted to the load is very small.

If only a very high magnetic flux density is desired, the harvesting time ($t_{harvest}$) would be too short to harvest sufficient power. Conversely, if $t_{harvest}$ is set to be long, the magnetic flux density decreases, resulting in a smaller magnitude of harvested power. In this paper, we analyze the relationship between $t_{harvest}$ and magnetic flux density from the perspective of core design. We then propose a design that can harvest the maximum power under given operating conditions.

A. DESIGN CONSIDERATION FOR THE CT

Before developing the optimal MEH design, it is important to discuss the perspective from which the existing core for a CT is designed. Although a CT and MEH have different objective functions, the design variables and their impact on the system are similar. Accordingly, it is necessary to understand the CT design to proceed with the optimal MEH design.

The CT model and equivalent circuit model can be expressed simply, as shown in green in Fig. 2(a) and Fig. 4. A current on the secondary side (i_{o_CT}) is generated by a current on the primary side (i_p) by Faraday's law. The value of the current on the primary side is calculated by measuring the voltage applied to the installed shunt resistor (R_{shunt}), as follows:

$$i_{o\_CT} = \frac{i_p}{N_2}, \quad i_p = \frac{N_2}{R_{shunt}} v_{o\_CT} \tag{1}$$

Equation (1) is derived for operating environments where the core is not saturated. Under heavy-load conditions where the core can become saturated, distortions can occur in the voltage waveform, leading to phase differences between voltage and current, as in [22], [23], and [24].

1) AIRGAP

When the core reaches saturation, no voltage is induced in the secondary, and the primary current cannot be calculated.

For this reason, in the case of CT, the core should be designed not to be saturated in the operating current range, as shown by the red line in Fig. 3. The B-H curve can be deformed by adding an airgap between the core, as shown in Fig. 5(a). When an airgap is added between the cores, the effective magnetic permeability of the cores changes, as described in [22]. Even if the airgap changes, the magnitude of B_{sat} does not change, but the magnitude of the magnetic field H reaching B_{sat} increases. Therefore, the slope of the B-H curve can be adjusted by changing the airgap, and the CT core can be designed so that it does not become saturated within the entire operating current range.

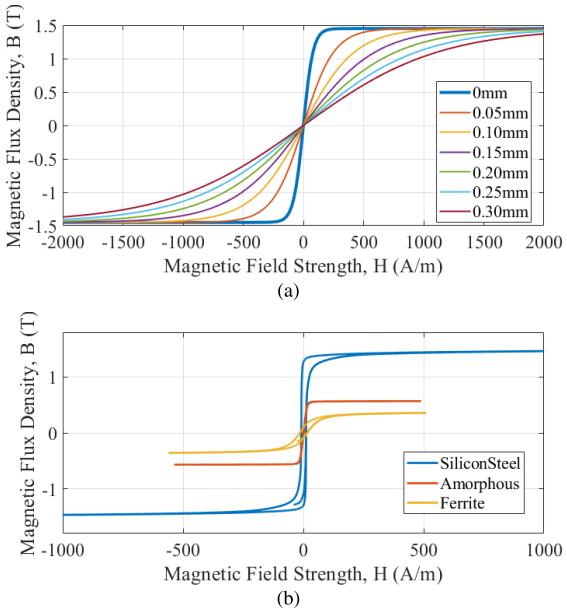

FIGURE 5. B-H curve characteristics according to core design. (a) B-H curve according to airgap. (b) B-H curve according to magnetic material. The slope of the B-H curve and the magnitude of the maximum magnetic flux density are very important in the design of the MEH system, as they affect the saturation of the core, the resulting secondary side voltage and current, and the output power.

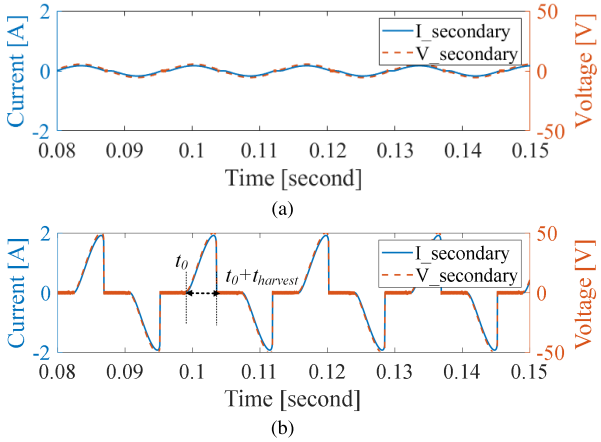

FIGURE 6. Waveforms of secondary voltage and current (a) when using a core for CT (b) when using a core for MEH. The secondary side voltage and current induced by a CT flow continuously across all sections because the core does not saturate. However, their magnitude is very small. In contrast, the secondary side voltage and current generated by a MEH are discontinuous due to the core's saturation in specific sections, but they have the advantage of being larger in magnitude.

2) SECONDARY TURNS (N_2) AND SHUNT RESISTANCE

The number of turns of the CT core is generally determined according to a specification of the CT. The primary-side current: secondary-side current ratio is set to 100:5, 200:5, or 60:1, and the number of turns is set to 20, 40, or 60 according to (1).

The shunt resistance for measuring the secondary side voltage is set for the proper sensitivity setting. The

sensitivity (S_p), which is an important CT specification, refers to its ability to accurately measure and transform the current flowing through a conductor to a lower, measurable level which is calculated as,

$$S_p = \frac{v_{o\_CT}}{i_p} = \frac{R_{Shunt}}{N_2} \tag{2}$$

The lower the sensitivity, the more accurately the current can be measured. However, a CT that is too sensitive may be more prone to saturation and other errors. It is important to choose a CT with the appropriate sensitivity for the specific application.

3) MAGNETIC MATERIAL

The linear range of the core can also be determined by the selection of magnetic material. Silicon steel, amorphous, and ferrite are commonly used materials for core production, and the B-H curve for each is shown in Fig. 5(b). Silicon steel has a saturation magnetic flux density much higher than amorphous or ferrite, but it becomes saturated much faster. Conversely, ferrite has a low saturation magnetic flux density, but has a wide linear range compared to other materials. In the case of CT, since linearity is more important than increasing the induced voltage, a material that can not be saturated in the entire region should be selected in consideration of the characteristics of each material and the linear range.

In summary, the key consideration when designing a CT core is to achieve linearity across all areas, ensuring that the core does not saturate. This design objective aims to enable accurate current measurement by extending the B-H curve and facilitating continuous current flow through the CT over a wide range, as depicted in Fig. 6(a). As seen in Fig. 6(a), the magnitudes of voltage and current are very small but continuous. Therefore, the power by CT in this case can be calculated very simply as,

$$p_{out} = \int_{t_0+T}^{T} v(t) \cdot i(t) \tag{3}$$

B. DESIGN CONSIDERATION FOR THE MEH

CTs must accurately measure continuous current, while MEHs aim to deliver maximum power to the connected load. To achieve high power delivery, it is necessary to have a high magnetic flux density under the same current conditions, as shown by the blue line in Fig. 3, and a longer time for power harvesting. In other words, the system should operate within a wide range of currents without saturation, as described in [25]. However, the magnetic flux density and the range of saturating current have an inverse relationship. It is essential to appropriately analyze their relationship and design the system with an optimal structure that allows for maximum power harvesting in the given environment.

In Figs. 6(a) and (b), the waveforms of secondary voltage and current are shown when utilizing a core with a gentle B-H curve slope (red line) and a steep B-H curve slope (blue line) of Fig. 3, respectively. Looking at Fig. 6(a), although the voltage and current are continuous, the magnitude of the induced voltage and current is very small, resulting in minimal harvested power (0.316 W). Conversely, in Fig. 6(b), due to the saturation of the core, voltage and current are induced only in certain regions, but their magnitudes are significantly larger, resulting in a much higher average harvested power of 21.43 W.

The characteristics of this B-H curve can be created depending on how the design parameters of the core are set. Fig. 5 shows the changes in the characteristics of the B-H curve as a result of varying the core's material and the air gap between cores. Therefore, the amount of power harvested can vary depending on how these design parameters are implemented.

In this paper, to maximize power harvesting, the relationship between magnetic flux density and the time during which power is harvested is analyzed to find the optimum point. The design variables of the core, such as the airgap, secondary turns, equivalent load impedance, and magnetic material, identified through the aforementioned analysis, are adjusted to implement this optimum point and design the system accordingly.

III. DESIGN OF MAGNETIC ENERGY HARVESTING SYSTEM

The harvesting power in the MEH system greatly varies depending on how the core is designed. The MEH core can be designed as shown in Fig. 7. The harvested power depends on the saturation state of the core and the harvesting time(t_h), as well as the voltage and current induced in the secondary side. In particular, t_h is determined by various design variables. This paper aims to calculate t_h, as indicated by the blue dotted line in Fig.7, using a mathematical approach and to analyze the trade-off relationship between t_h and flux density to propose a core design that can harvest maximum power. Especially, while previous studies simply designed the airgap between cores to prevent saturation over the entire operating range, this study suggests a method for selecting an airgap that allows for maximum power harvesting, even if saturation occurs in certain ranges.

To derive the relationship, the harvested power equation when using the MEH core is first obtained, and the harvesting time and harvested power according to each parameter change are analyzed.

A. HARVESTING TIME AND POWER BY THE MEH

Figure 8 shows a simplified equivalent circuit of the MEH system. R_{L_eq} represents the processing of the rectifier and dc-dc converter as an equivalent model. First, the secondary current ($i_s(t)$) flowing through the core by the primary current ($i_p(t)$) is calculated as follows [20]:

$$i_s(t) = \frac{i_p(t)}{N_2} - i_m(t) = \frac{I_p \sin(\omega t)}{N_2} - i_m(t) \tag{4}$$

Because the magnetizing inductor L_m ideally only repeats energy storage and release, the average current flowing

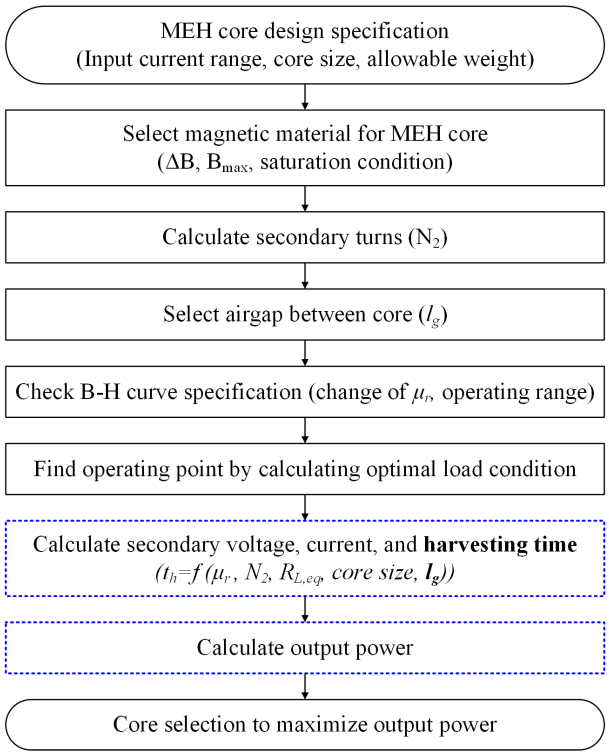

FIGURE 7. MEH core design flowchart. In this paper, the influence of various core design parameters on harvesting time is analyzed, and a method to derive the output power based on these parameters is proposed as indicated by the blue dotted line.

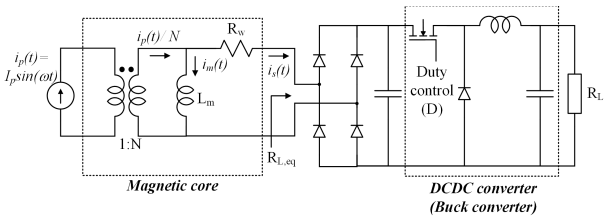

FIGURE 8. Equivalent circuit of the MEH system including the converter and rectifier. Unlike CTs, at the back of the core in MEH systems, there is a circuit for power conversion and a load demanding several to tens of watts connected.

through this inductor ($i_m(t)$) becomes zero. Therefore, the average value of the secondary current is calcualted as,

$$\begin{aligned} i_{s,avg} &= \frac{2}{T}\int_{t_0}^{t_0+t_h}\left(\frac{I_p\sin(\omega t)}{N_2} - i_m(t)\right)dt \\ &= \frac{2}{T}\int_{t_0}^{t_0+t_h}\frac{I_p\sin(\omega t)}{N_2}dt \\ &= \frac{2I_p}{\pi N_2}\sin\left(\omega t_0+\frac{\omega t_h}{2}\right)\sin\left(\frac{\omega t_h}{2}\right) \end{aligned} \tag{5}$$

. Here, power can be harvested only during the interval from t_0 to $(t_0 + t_h)$, due to the saturation of the core, as shown in Fig. 6(b). The integration interval is set accordingly.

The induced voltage on the secondary side is generated by the magnetic flux linkage and can be calculated as follows.

$$\int_{t_0}^{t_0+t_h} v_s(t)dt = 2B_{sat}A_cN_2 \tag{6}$$

Alternatively, the voltage on the secondary side $v_s(t)$ can be expressed, as shown in Fig. 8.

$$v_s(t) = i_s(t)\left(R_w + R_{L,eq}\right) \tag{7}$$

By utilizing (4), (6), and (7), the harvesting interval t_h can be derived using the following:

$$\begin{aligned} \int_{t_0}^{t_0+t_h} i_s(t)dt &= \int_{t_0}^{t_0+t_h}\frac{I_p\sin(\omega t)}{N_2}dt = \frac{2B_{sat}A_cN_2}{R_w+R_{L,eq}} \\ &= \frac{2I_p}{\omega N_2}\left(\sin(\omega t_0+\frac{\omega t_h}{2})\sin(\frac{\omega t_h}{2})\right) \end{aligned} \tag{8}$$

Taking t_0 as the reference point 0, the t_h can be solved as follows.

$$t_h = \frac{2}{\omega}\sin^{-1}\left(N_2\sqrt{\frac{A_cB_{sat}\omega}{I_p\left(R_w+R_{L,eq}\right)}}\right) \tag{9}$$

The averaged power harvested ($P_{o,avg}$) in Fig. 8 is calculated as, [10], [20] with (5), (6), and (8).

$$\begin{aligned} P_o &= v_{s,avg}\cdot i_{s,avg} \\ &= v_{s,avg}\left(\frac{2}{T}\int_{t_0}^{t_{sat}}\frac{I_p\sin(\omega t)}{N}dt\right) \\ &= \frac{2I_p}{\pi}\frac{R_L\left(B_{sat}A_c\right)}{R_L+R_w}\frac{\cos(\omega t_0)-\cos(\omega t_0+\omega t_{sat})}{t_{sat}} \end{aligned} \tag{10}$$

When we substitute (9) into (10), we can calculate the harvested power, including the saturation region.

The harvested power through (9) and (10) is influenced by various factors such as the primary current, the number of turns in the core, the equivalent load resistance, the core structure and the maximum magnetic flux density. This relationship is highly complex, and it requires an optimal design process tailored to the characteristics of the power line where the core is installed.

The number of turns required to achieve maximum power harvesting varies depending on the current magnitude in the power line, and correspondingly, an optimal load value exists, which can be observed in Fig. 9. Figure 9 presents the results obtained through the FEM and circuit simulations. Figures 9(a) and (b) illustrate the optimal load resistance with respect to the primary input current and the number of turns and the optimal number of turns with respect to the primary input current and load resistance, respectively. The optimal equivalent load resistance $R_{L,eq}$ can be adjusted through the duty control of the DC-DC converter, as shown in [26], [27], and [28].

The harvested power, which varies due to various parameters, has been confirmed by (9) and (10); however, these studies do not consider the airgap of the core. This has not been shown in other MEH-related papers.

Changes in the airgap of the core result in the modification of the effective permeability and cause variations in the slope of the B-H curve, as depicted in Fig. 5(a). Note that the maximum magnetic flux density (B_{sat}) remains unchanged. As a result, variations in the airgap affect the time during which power is harvested and also influence the harvested

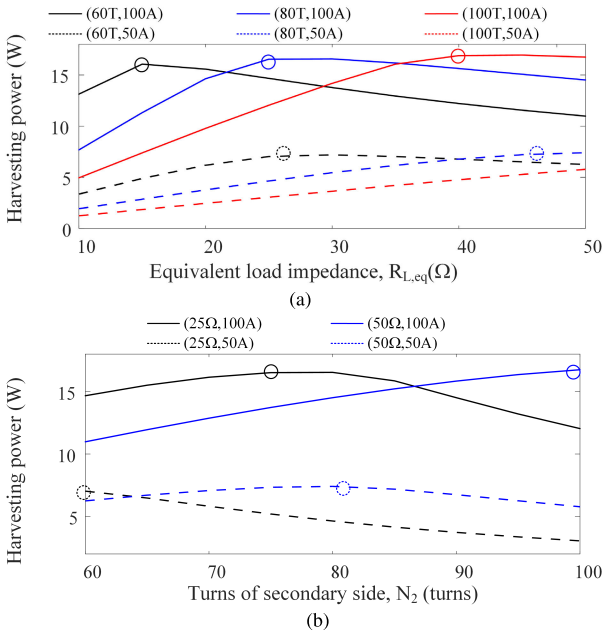

FIGURE 9. Harvesting power according to (a) equivalent load impedance and (b) the number of the secondary turns. Due to the complex relationships between design variables, the optimal core design varies depending on the input current conditions and the size of the equivalent load resistance. It is essential to understand these relationships to design a core capable of harvesting maximum power.

power. Consequently, (9) and (10) should be derived again by incorporating the airgap parameter to accurately account for its impact.

B. HARVESTING TIME ACCORDING TO AIRGAP OF MEH CORE

The MEH core is mostly made in a cutting-core design and produced in a clip form for easy installation on power lines, as shown in Fig. 10(a). As a result, an airgap occurs between the cut surfaces of the core which consequently affects the characteristics of the B-H curve of the core, as shown in Fig. 10(b). Even with changes in the airgap, the maximum magnetic flux density remains the same. However, the magnetic field intensity required to reach the maximum value differs, affecting the amount of harvested power. Nevertheless, (9) and (10) do not consider the effect that changes in the airgap have on the amount of harvested power.

To improve the equation for harvested power and harvesting time, we first analyze the relationship between the magnetic field intensity and the secondary current with respect to the air gap through waveform analysis. The black, blue, and red lines in Fig. 10 represent cases where the airgap between the cores is 0.3, 0.1, and 0mm, respectively. When the air gap is 0.3mm, the magnitude of $B(t)$ with respect to the input current $i_p(t)$ does not exceed B_{sat} (saturation level). As a result, the secondary current $i_s(t)$ appears continuously. However, for the blue and red graphs, as the airgap decreases, the slope of the B-H curve increases, as shown in Fig. 10(b). For the same input current, a smaller airgap leads to a faster

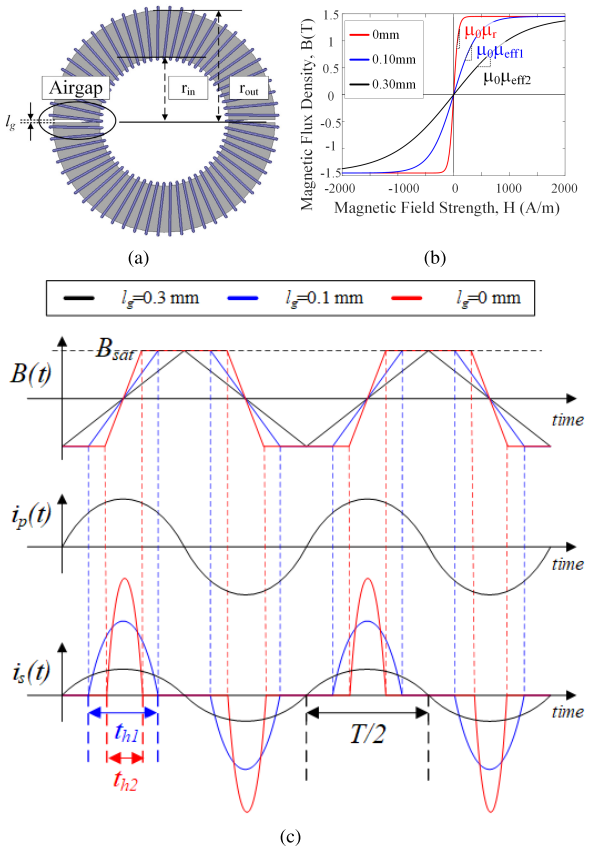

FIGURE 10. Core characteristics change according to the airgap. (a) Schematic of MEH core model, (b) slope change of the B-H curve according to the airgap, and (c) magnetic flux density, primary current, and secondary current according to the airgap. The slope of the B-H curve changes depending on the airgap, which in turn affects the harvesting time and the maximum value of the secondary-side current.

approach to B_{sat}, resulting in a larger saturation region. Consequently, we can observe that as the airgap decreases, the harvesting time gradually decreases from $T/2$ to t_{h1} and t_{h2} at the secondary current waveform.

To formulate the harvested power and harvesting time based on the airgap, first, we calculate the effective permeability of the core corresponding to the air gap as follows [29]:

$$N_2 \Delta I_s = \frac{\Delta B}{\mu_0 \mu_{eff}} l_e = \frac{\Delta B}{\mu_0 \mu_r} l_c + \frac{\Delta B}{\mu_0} l_g \tag{11}$$

$$\mu_{eff} = \frac{\mu_r}{\frac{l_c}{l_c+l_g} + \frac{l_g}{l_c+l_g}\mu_r} \approx \frac{\mu_r}{1+\frac{l_g}{l_c}\mu_r} \quad \left(l_c \gg l_g\right), \tag{12}$$

where μ_r, l_g, and l_c represent the permeability of the core, airgap length, and effective magnetic core length, respectively.

When incorporating μ_e to linearize the B-H curve, it becomes as shown in Fig. 10(b). The slope of each B-H curve is represented by $\mu_0\mu_{eff}$, and as l_g (airgap length) increases, the slope decreases. When l_g is 0, the slope becomes $\mu_0\mu_r$, which is the largest slope possible.

To interpret the harvesting time t_h with consideration of μ_{eff}, we can apply Faraday's law and Ampere's circuital law again, leading to the following expansions of

equations (6), (7), and (8):

$$\int_{t_0}^{t_0+t_h} \frac{I_p \sin(\omega t)}{N_2} dt = \frac{N_2 (\Phi(t_0+t_h) - \Phi(t_0))}{R_w + R_{L,eq}} = \frac{N_2 I_p (\sin(\omega t_0 + \omega t_h) - \sin(\omega t_0))}{\left(\frac{\pi(d_{out}+d_{in})-l_g}{\mu_0 \mu_{eff} A_c} - \frac{l_g}{\mu_0 A_c}\right)(R_w + R_{L,eq})} \tag{13}$$

. If we take t_0 as the reference point and solve the integration, the harvesting time t_h is derived as follows:

$$t_{h,prop} = \frac{2}{\omega} \cos^{-1}\left[\frac{2(R_w + R_{L,eq})}{\omega {N_2}^2} \times \left(\frac{\pi(r_{out}+r_{in})-l_g}{\mu_0 \mu_{eff} A_c} - \frac{l_g}{\mu_0 A_c}\right)\right], \tag{14}$$

where μ_{eff} is calculated by substituting (12). Furthermore, the harvested power can be calculated using $t_{h,prop}$ instead of t_h in (10). Here, the maximum value of $t_{h,prop}$ is a half cycle.

The proposed (14) differs from the conventional (9) in that it not only accounts for the load resistance and the number of turns but also the size of the core and the airgap between the split cores. Therefore, it enables the calculation of power considering core saturation due to the airgap, allowing for an optimal design.

To validate the proposed equation, simulations were performed using ANSYS MAXWELL and MATLAB Simscape to observe the secondary current and the harvested power with varying airgap sizes, as shown in Fig. 11.

Firstly, when the airgap is 0.3 mm, the core does not reach saturation, and the secondary current exhibits a continuous waveform. In this case, the harvesting time (t_h) is $T/2$ (8.3 msec). Although power can be harvested at all intervals, the harvested power is minimal since the magnetic flux density cannot be significant for the given primary current. Secondly, with an airgap of 0.1 mm, the core reaches saturation, resulting in a discontinuous waveform for the secondary current. In this case, t_h is 5.9 milliseconds. Despite the discontinuous waveform, a higher magnetic flux density is achieved compared to the 0.3mm airgap, leading to a higher average power harvested. Lastly, with no airgap, the core saturates even faster, resulting in the shortest t_h of 4.5 milliseconds. In this case, the fastest change in magnetic flux density for the given primary current induces a significant voltage in the secondary, leading to the highest average power harvested.

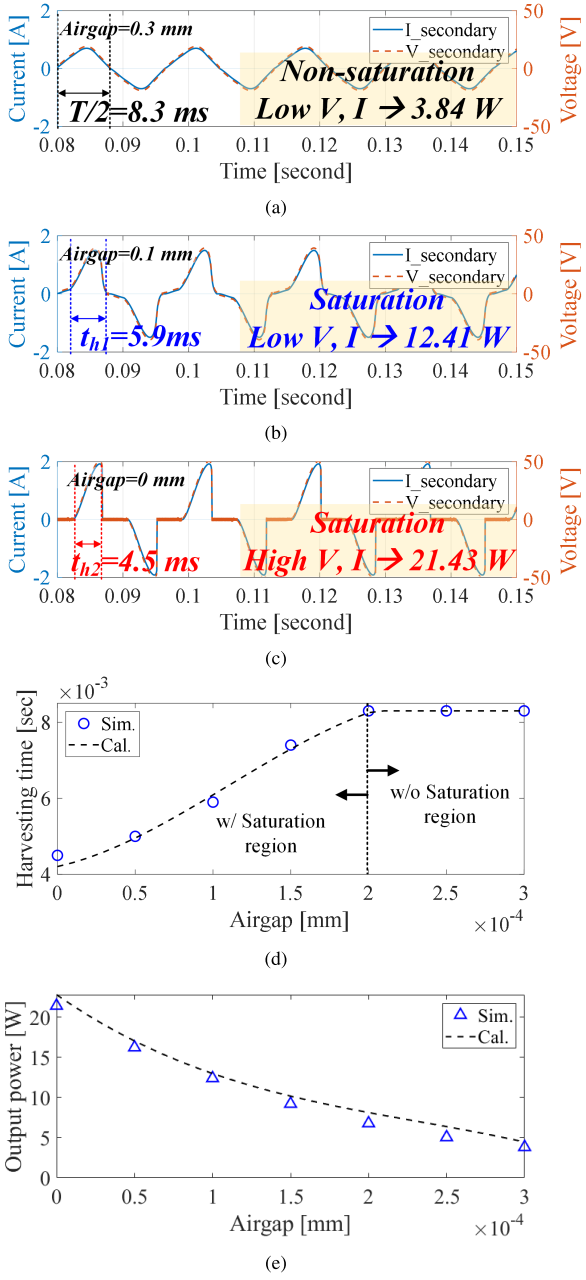

FIGURE 11. Harvesting power change when saturation period is adjusted through airgap control under the same conditions: (a) Airgap = 0.3 mm, (b) Airgap = 0.1 mm, and (c) Airgap = 0 mm. (d) Harvesting time according to airgap. (e) Output power according to airgap. When the airgap is smaller, the amount of power harvested increases, but there is a trade-off relationship as the maximum voltage and current significantly increase.

IV. OPTIMAL DESIGN OF THE MEH FOR MAXIMUM POWER

The power harvested using an MEH varies significantly depending on the core design parameters, such as the air gap between the cross-sectional area of the core, the secondary turns of the core, and the equivalent resistance, as shown in (14) and (10). Additionally, the harvested power also varies based on the current level of the power line where the core is installed, and optimal core designs exist for each current level, as shown in Fig. 9 and Fig. 11. In this section, we propose optimized MEH models depending on the primary current level using the equations for harvested power based on the proposed harvesting time that varies depending on the airgap, along with FEM and circuit simulation results.

In most power conversion systems, the efficiency of power transfer is the most important factor, and many studies strive to improve system efficiency. However, the MEH system discussed in this paper harvests power using the magnetic field generated by power lines carrying very

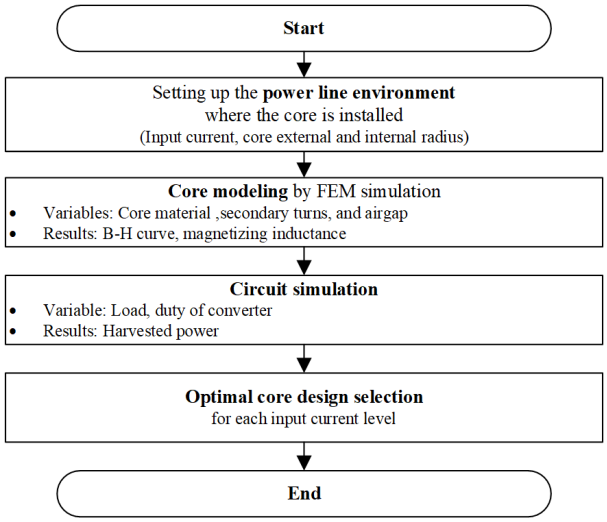

FIGURE 12. Simulation procedure for optimal core design for the input current. To examine the harvested power according to various design parameter changes, simulations were conducted using ANSYS's MAXWELL software.

high power, making it impossible to calculate the power transfer efficiency as the primary side energy cannot be quantified. Instead, the most crucial factor in MEH systems is the magnitude of the harvested power. Some studies focus on reducing volume and mass while harvesting the same power, focusing on power density [W/cm^3] or specific power [W/kg], which is the power harvested per unit volume or mass, respectively. However, this paper fixed the size of the core, which significantly affects the system's volume and weight, and set the design variables as the number of turns, air gap, and equivalent resistance. The objective function was designed to maximize the output power according to the input current.

The design parameters include the airgap between the cross-sectional area of the core, the number of secondary turns, and the equivalent load resistance, as shown in Table 1. We performed optimization of the design by varying the input current from 50 Arms to 150 Arms in steps of 25 Arms.

The simulation process is illustrated in Fig. 12, and the variable conditions used in the simulation are listed in Table 1. For the FEM and circuit simulation, ANSYS's MAXWELL and MATLAB's Simscape were used, respectively. A simulation analysis was conducted for a total of 1080 core models. The corresponding results are summarized in Fig. 13. The harvested power according to an equivalent load resistance, to secondary side turns, and to the airgap is displayed as (a)-(e), (f)-(j), and (k)-(o), respectively.

As analyzed through the aforementioned mathematical equations, the load resistance and secondary side turns do not exhibit a simple linear relationship with the harvested power. Regarding secondary side turns, although not strictly linear, it is observed that higher power can be harvested with more turns. However, the magnitude of the power saturates at certain turn counts. As the number of turns in the core

TABLE 1. Design parameters for the simulation.

Parameters	Start	Stop	Step
Input current	50 A	150 A	25 A
Airgap	0 mm	0.05 mm	0.01mm
Turns of secondary side	40 turns	140 turns	20 turns
Equivalent load impedance	10 Ω	150 Ω	25 Ω
Total number of model		1080	

TABLE 2. Optimal MEH models according to input current conditions.

I_p [A]	Airgap [mm]	N_2 [turns]	$R_{L,eq}$ [Ω]	Power [W]
50	0	60	85	7.56
75	0	80	60	12.52
100	0	80	35	17.30
125	0	80	10	21.64
150	0	80	10	26.75

increases, factors such as weight, cost, and winding loss also increase, necessitating the selection of an optimal turn count to harvest the desired power. Regarding the airgap, the simulation results indicate that the maximum power can be harvested when the airgap is zero in all scenarios.

In designing the MEH system, it is crucial to first examine the environment in which the core will be installed along the power lines. Next, by simulating and determining the required turn count, the core can be designed. In this process, the airgap that can occur on the cross-sectional plane of the core is designed to be as close to zero as possible. Finally, by adjusting the converter duty cycles and other factors in the power circuit, the equivalent load resistance is matched to attain the maximum harvested power. Figure 14 shows the maximum power available to harvest for each input current through this process.

V. EXPERIMENTAL VERIFICATION

A. EXPERIMENT PROCESS AND RESULTS

For experimental verification of the proposed MEH core design, an MEH system was implemented, as shown in Fig. 15. The core was made of a cutting core for easy installation on the power line. When the core is cut, an airgap is inevitably created, and the performance is lower than that of the ring core. However, Ferraris Power, Inc. has the technology to minimize the loss during core cutting, and they can make the airgap nearly zero, i.e., almost identical to the ring core. Experiments were conducted based on Ferraris Power, Inc.'s 'Tolenoid C model'.

As shown in Table 3, the experiment was divided into two types according to the input current conditions. First, when the input current is 50 A, the harvesting power was confirmed according to the change in the equivalent load impedance. At this time, the number of turns of the core and the airgap were fixed at 60 turns and 0 mm, respectively.

The experimental results are shown in Fig. 16 with an input current of 50 Arms and Fig. 17 with an input

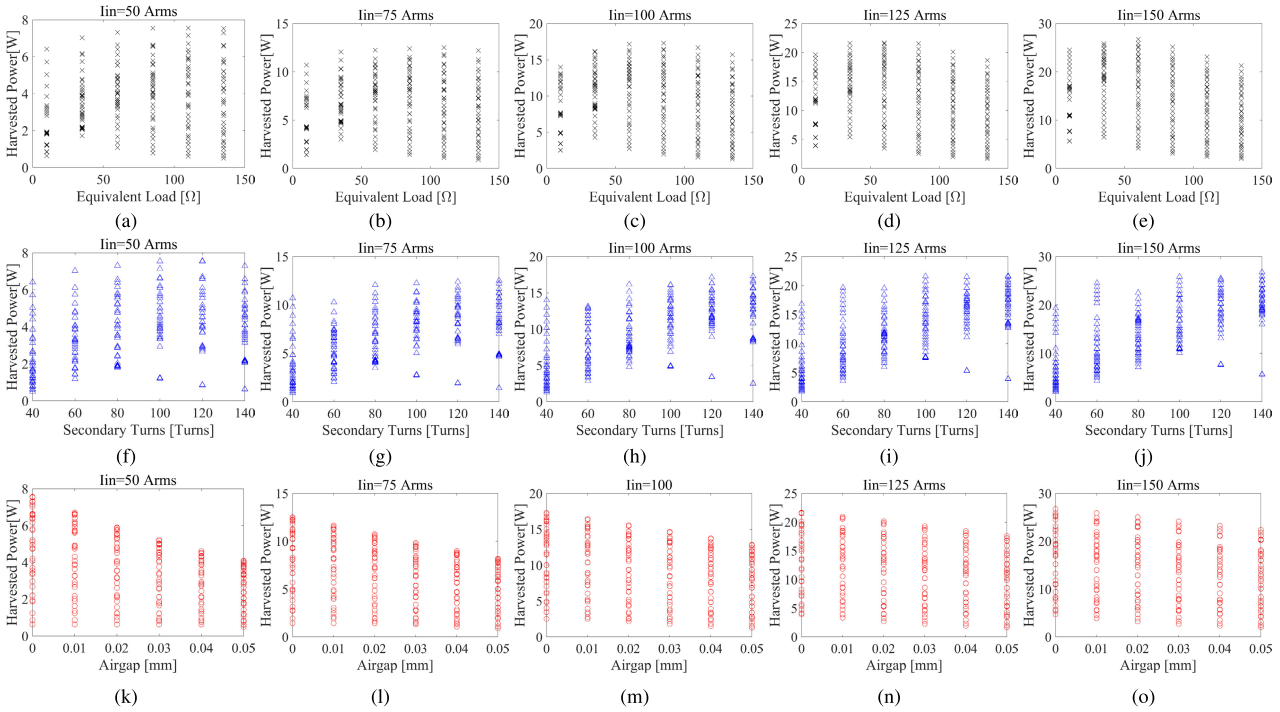

FIGURE 13. Simulation results for each input current. (a)-(e) Relationship between equivalent load resistance and harvested power. (f)-(j) Relationship between secondary turns and harvested power. (k)-(o) Relationship between the airgap and harvested power. Simulations were carried out for a total of 1080 core designs, and through these results, the design parameters that can harvest the maximum power for each input current were determined. The determined design parameters are summarized in TABLE 2.

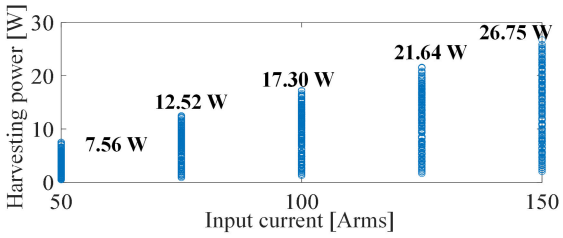

FIGURE 14. Maximum power by the MEH at a given input current level.

TABLE 3. Experiment setup.

Parameters	Exp.1	Exp.2
Input current	50 A	150 A
Turns of secondary side	60 turns	80 turns
Equivalent load impedance	(60, 85, 110) Ω	10 Ω
Airgap	0 mm	(0, 0.05, 0.1) mm

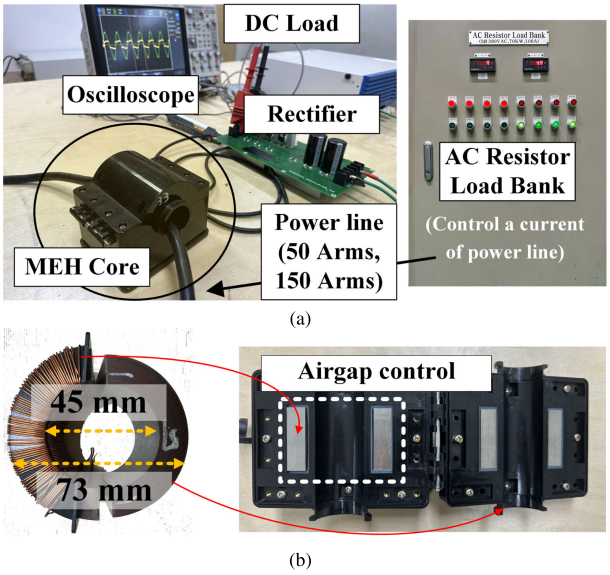

FIGURE 15. Experiment setup for the MEH system using Ferraris Power, Inc.'s 'Tolenoid C' model. The core material is silicon steel, manufactured using a rolling method. The case was designed to minimize the air gap between the cutting core. The air gap variation experiment was conducted by adjusting the gap using Kapton tape attached between the core.

current of 150 Arms. The waveform was measured using an oscilloscope from Keysight. The yellow and blue colors represent the secondary side voltage and current of the core, respectively, while the green and purple colors show the values of the rectified voltage and current. In the bottom right corner, the output power measured using an electronic load has been added.

As a result of the experiment, as shown in Fig. 14 and Table 2, it was confirmed that the highest power was obtained with 8.4 W when the equivalent load impedance was 85 Ω. When the load was set to 85 Ω, the harvesting time was shorter compared to other load conditions, but it was able to harvest a large amount of power due to the large secondary side current.

Second, when the input current is 150 A, the harvesting power was confirmed according to the addition of the airgap between the cores, and the experimental results are

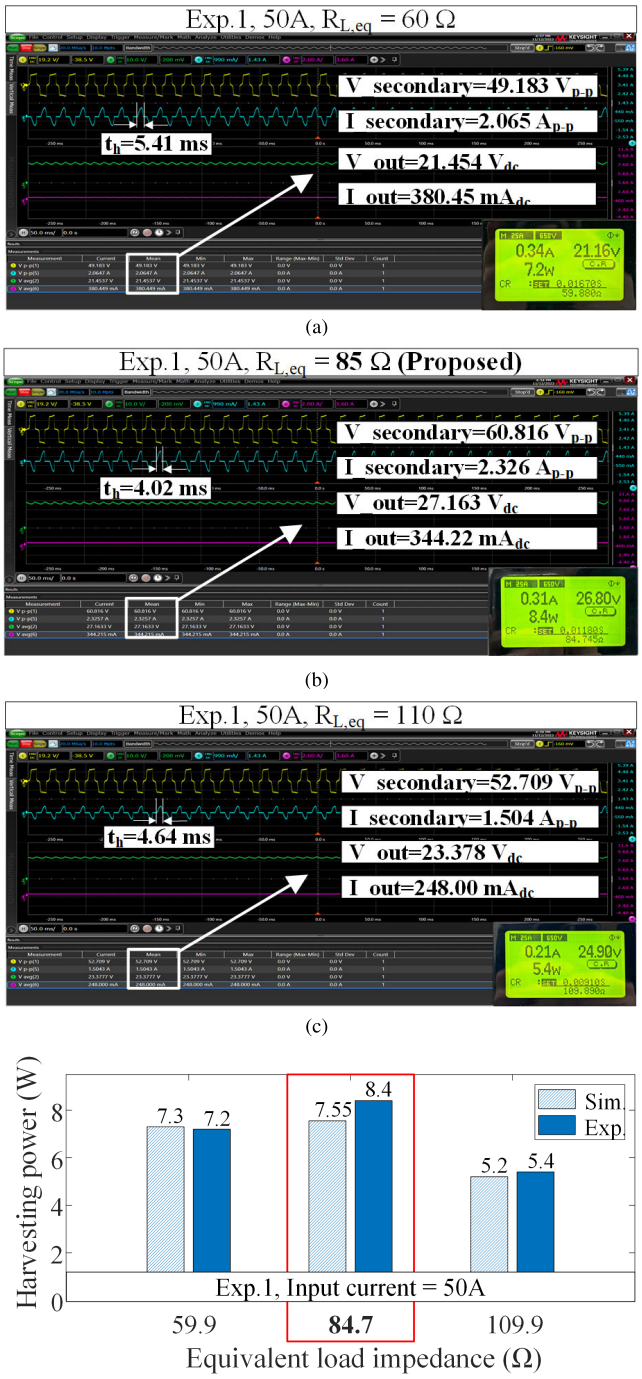

FIGURE 16. Experimental results when the input current is 50 Arms (Exp. 1) (a) $R_{L,eq}$ = 59.9 *ohm* (b) (Proposed) $R_{L,eq}$ = 84.7 *ohm* (c) $R_{L,eq}$ = 109.9 *ohm* (d) Output power with load change.

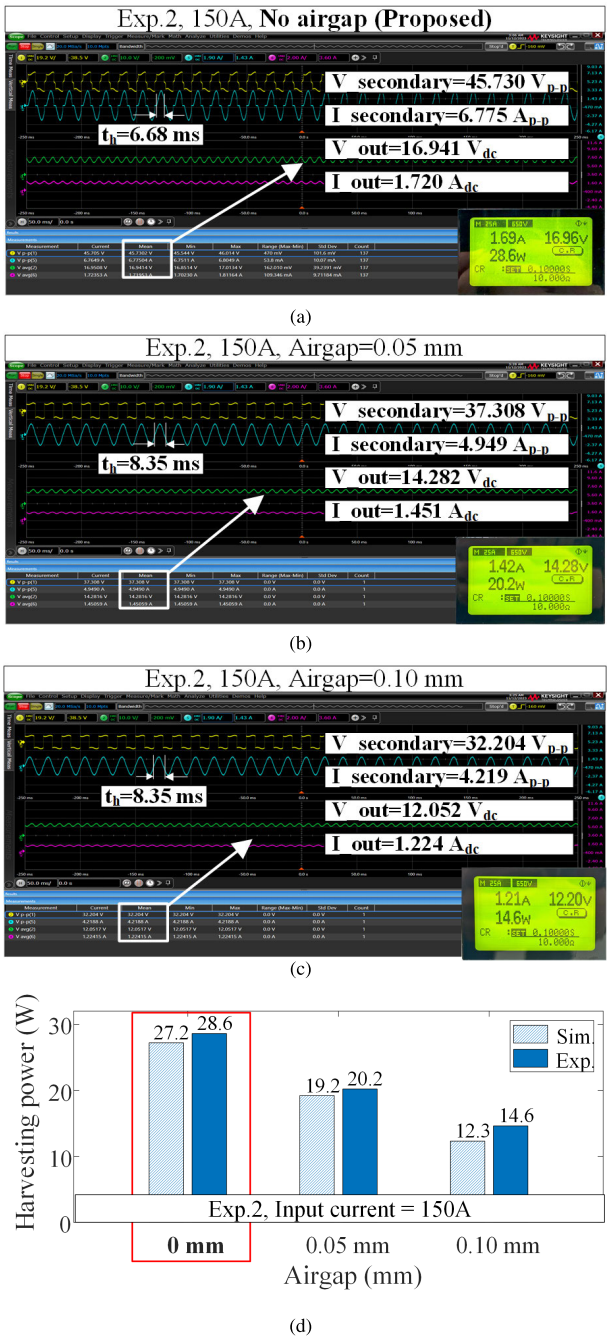

FIGURE 17. Experimental results when the input current is 150 Arms (Exp. 2) (a) (Proposed) NO airgap (b) Airgap = 0.05 mm (c) Airgap = 0.10 mm (d) Output power with airgap change.

shown in Fig. 17. At this time, the number of core turns and equivalent load resistance were fixed at 80 turns and 10 Ω, respectively. The resulting waveforms are shown in Figs. 17(a), (b), and (c), and the results are summarized in (d). When the airgap is set to 0.1mm, as shown in Fig. 17(b) and (c), the power can be harvested from all areas without saturation in the operating area. However, since the rate of change of the magnetic field compared to the same change of current is reduced, a large current can not be induced on the secondary side. However, when the airgap is set to 0 mm, as shown in Fig. 17(a), the core is saturated in a specific section; therefore, power can be harvested only in a narrow area, but the magnetic field change rate increases, so a large current is induced in the secondary side and higher power can be harvested. As a result of the experiment, as shown in Fig. 14 and Table 2, it was confirmed that

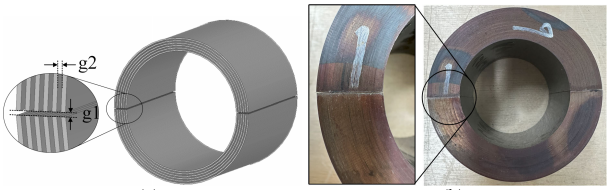

FIGURE 18. Airgaps that can occur during the core manufacturing process. (a) Simulation model. (b) Real model. The air gap (g1) between the cut cores is important, but minimizing the air gap (g2) that can occur during the rolling process of the core is also crucial for achieving better performance.

TABLE 4. Optimal MEH models according to input current conditions.

Previous studies	Max. Power	Magnetic saturation effect	Power analysis based on changes in the airgap
[9]	5.2 W @ 4 Arms	O	X
[10]	3.0 W @ 50 Arms	O	X
[15]	2.5 W @ 200 Arms	X	X
[17]	10.3 mW @ 14 Arms	X	X
[20]	88 mW @ 12 Arms	O	X
[21]	14.3 W @ 70 Arms	O	X
This paper	8.0 W @ 50 Arms 28 W @ 150 Arms	O	O

the highest power of 28.6 W was obtained when the airgap was 0 mm.

B. CORE MANUFACTURING METHOD FOR HIGH POWER HARVESTING CHARACTERISTICS

To achieve the desired power characteristics, precise core manufacturing is essential. Typically, cores are made by winding steel sheets in rolled form. Once wound to the desired size, the core is cut and separated into a sectional form, as shown in Fig. 18, for easy installation on power lines. Within this manufacturing process, there are two types of airgaps that can occur, represented as g_1 and g_2 in Fig. 18(a).

Firstly, g_1 refers to the cutting loss that can occur during the process of cutting the core. Minimizing this loss is crucial when designing the core. There are several methods for cutting cores, including cutting with a saw, wire, or diamond, or using high water pressure. Detailed methods for minimizing cutting losses are described in [25]. Secondly, the gap indicated as g_2 in Fig. 18(a) represents the gap between thin steel sheets that can occur when they are wound into multiple turns. Although this gap is very small, it significantly influences the power characteristics of the core. As a consequence, to minimize this gap, we applied a technique involving heat treatment and impregnation of the rolled magnetic alloy during the core manufacturing process. A core obtained through this manufacturing process is illustrated in Fig. 18(b), where g_1 and g_2 have been minimized to maximize the power characteristics. Detailed information on such manufacturing techniques is explicitly described in [25] and [30].

VI. CONCLUSION AND DISCUSSION

As a power supply, MEHs should be designed from a different perspective than CTs used for accurate current measurement. In this paper, the performance indicators of an MEH and CT were mathematically analyzed, and design considerations were discussed in comparison with a CT. In the case of CT, the core is designed not to saturate in all areas, so the voltage and current have a continuous sine wave form. However, in the case of MEH, since the core should be designed to maximize the power delivered to the secondary side, the core is saturated in a certain period and the voltage and power induced to the secondary side have nonlinear characteristics. Among several core design variables, the change in characteristics of the core according to the airgap between the cut surfaces of the core was analyzed in this paper, and the relationship between the airgap and energy harvesting time was proposed to have a B-H curve close to the step function for maximum harvesting power. In addition, by analyzing the harvesting power for various design variables of the MEH as well as the airgap, a design parameter set under a given input current condition was presented. Through experiments, we verified that the proposed MEH could harvest 28 W of power under 150 A.

In this study, we successfully harvested tens of watts of power using a single MEH core. In the future, we plan to conduct research on methods and system optimization for harvesting more power using multiple cores. Additionally, we plan to verify the stability of the MEH system through an analysis of the impact on power lines when multiple cores are installed.

ACKNOWLEDGMENT

The authors would like to thank Ferraris Power Inc., for providing the core, patents, and experimental environment for the article and also would like to thank the technical support from ANSYS Korea.

REFERENCES

[1] *Transmission Line Inspection Robot 'IR-TLI100' by SHENHAO*. Accessed: Aug. 14, 2023. [Online]. Available: https://www.shenhaorobotics.com/transmission-line-inspection-robot/

[2] *Transmission Line Conductor Monitor by LINDSEY System*. Accessed: Aug. 14, 2023. [Online]. Available: https://lindsey-usa.com/sensors/transmission-line-monitor/

[3] *Overhead Line Sensor by InHand Networks*. Accessed: Aug. 14, 2023. [Online]. Available: https://www.inhandnetworks.com/solutions/IWOS/overhead-line-sensor.html

[4] A. Andrawes, R. Nordin, and M. Ismail, "Wireless energy harvesting with amplify-and-forward relaying and link adaptation under imperfect feedback channel," *J. Telecommun., Electron. Comput. Eng.*, vol. 10, no. 3, pp. 83–90, Aug. 2018.

[5] A. Andrawes, R. Nordin, and M. Ismail, "Energy harvesting with cooperative networks and adaptive transmission," in *Proc. IEEE Jordan Conf. Appl. Electr. Eng. Comput. Technol. (AEECT)*, Oct. 2017, pp. 1–6.

[6] Z. Albataineh, A. Andrawes, N. Abdullah, and R. Nordin, "Energy-efficient beyond 5G multiple access technique with simultaneous wireless information and power transfer for the factory of the future," *Energies*, vol. 15, no. 16, p. 6059, Aug. 2022.

[7] A. Andrawes, R. Nordin, and M. Ismail, "Wireless energy harvesting with cooperative relaying under the best relay selection scheme," *Energies*, vol. 12, no. 5, p. 892, Mar. 2019.

[8] K. Tashiro, H. Wakiwaka, S.-I. Inoue, and Y. Uchiyama, "Energy harvesting of magnetic power-line noise," *IEEE Trans. Magn.*, vol. 47, no. 10, pp. 4441–4444, Oct. 2011.
[9] S. Yuan, Y. Huang, J. Zhou, Q. Xu, C. Song, and P. Thompson, "Magnetic field energy harvesting under overhead power lines," *IEEE Trans. Power Electron.*, vol. 30, no. 11, pp. 6191–6202, Nov. 2015.
[10] Z. Liu, Y. Li, H. Yang, N. Duan, and Z. He, "An accurate model of magnetic energy harvester in the saturated region for harvesting maximum power: Analysis, design, and experimental verification," *IEEE Trans. Ind. Electron.*, vol. 70, no. 1, pp. 276–285, Jan. 2023.
[11] W. He, P. Li, Y. Wen, J. Zhang, A. Yang, and C. Lu, "A noncontact magnetoelectric generator for energy harvesting from power lines," *IEEE Trans. Magn.*, vol. 50, no. 11, pp. 1–4, Nov. 2014.
[12] Z. Wang, J. Hu, J. Han, G. Zhao, J. He, and S. X. Wang, "A novel high-performance energy harvester based on nonlinear resonance for scavenging power-frequency magnetic energy," *IEEE Trans. Ind. Electron.*, vol. 64, no. 8, pp. 6556–6564, Aug. 2017.
[13] G. A. Covic and J. T. Boys, "Inductive power transfer," *Proc. IEEE*, vol. 101, no. 6, pp. 1276–1289, Jun. 2013.
[14] S. Huh, B. Park, S. Choi, Y. Shin, H. Kim, J. Kim, J. Park, D. Park, and S. Ahn, "Transmitter coils selection method for wireless power transfer system with multiple transmitter coils and single receiver coil," *IEEE Trans. Power Electron.*, vol. 38, no. 3, pp. 4092–4109, Mar. 2023.
[15] L. Du, C. Wang, X. Li, L. Yang, Y. Mi, and C. Sun, "A novel power supply of online monitoring systems for power transmission lines," *IEEE Trans. Ind. Electron.*, vol. 57, no. 8, pp. 2889–2895, Aug. 2010.
[16] W. Wang, X. Huang, L. Tan, J. Guo, and H. Liu, "Optimization design of an inductive energy harvesting device for wireless power supply system overhead high-voltage power lines," *Energies*, vol. 9, no. 4, p. 242, Mar. 2016. [Online]. Available: https://www.mdpi.com/1996-1073/9/4/242
[17] R. H. Bhuiyan, R. A. Dougal, and M. Ali, "A miniature energy harvesting device for wireless sensors in electric power system," *IEEE Sensors J.*, vol. 10, no. 7, pp. 1249–1258, Jul. 2010.
[18] Y. H. Wu, X. Z. Dong, and S. Mirsaeidi, "Modeling and simulation of air-gapped current transformer based on Preisach theory," *Protection Control Mod. Power Syst.*, vol. 2, no. 1, pp. 1–11, Dec. 2017.
[19] P. Dworakowski, A. Wilk, M. Michna, B. Lefebvre, F. Sixdenier, and M. Mermet-Guyennet, "Effective permeability of multi air gap ferrite core 3-phase medium frequency transformer in isolated DC–DC converters," *Energies*, vol. 13, no. 6, p. 1352, Mar. 2020.
[20] J. Moon and S. B. Leeb, "Analysis model for magnetic energy harvesters," *IEEE Trans. Power Electron.*, vol. 30, no. 8, pp. 4302–4311, Aug. 2015.
[21] B. Park, S. Huh, J. Kim, H. Kim, Y. Shin, S. Woo, J. Park, A. Brito, D. Kim, H. H. Park, O. Jeong, J.-I. Koo, and S. Ahn, "The magnetic energy harvester with improved power density using saturable magnetizing inductance model for maintenance applications near high voltage power line," *IEEE Access*, vol. 9, pp. 82661–82674, 2021.
[22] M. K. Kazimierczuk, *High-Frequency Magnetic Components*. Hoboken, NJ, USA: Wiley, 2009.
[23] S. Ziegler, R. C. Woodward, H. H.-C. Iu, and L. J. Borle, "Current sensing techniques: A review," *IEEE Sensors J.*, vol. 9, no. 4, pp. 354–376, Apr. 2009.
[24] A. Hooshyar and M. Sanaye-Pasand, "CT saturation detection based on waveform analysis using a variable-length window," *IEEE Trans. Power Del.*, vol. 26, no. 3, pp. 2040–2050, Jul. 2011.
[25] J.-I. Koo, "Current transformer device," U.S. Patent 10 453 604, Oct. 22, 2019.
[26] W. X. Zhong and S. Y. R. Hui, "Maximum energy efficiency tracking for wireless power transfer systems," *IEEE Trans. Power Electron.*, vol. 30, no. 7, pp. 4025–4034, Jul. 2015.
[27] C. Ma, X. Qu, Y. Li, and J. Liu, "Single-stage active rectifier with wide impedance conversion ratio range for inductive power transfer system delivering constant power," *IEEE Trans. Power Electron.*, vol. 38, no. 6, pp. 7877–7890, Jun. 2023.
[28] S. Ghadeer, N. Rezaei-Hosseinabadi, A. Tabesh, and S. A. Khajehoddin, "Improving wireless power transfer efficiency considering rectifier input impedance and load quality factor," *IEEE Access*, vol. 11, pp. 61738–61747, 2023.
[29] V. C. Valchev and A. Van den Bossche, *Inductors and Transformers for Power Electronics*. Boca Raton, FL, USA: CRC Press, 2018.
[30] *Contactless Power Supply Solution'Tolenoid C' by Ferraris Power Inc.* Accessed: Aug. 14, 2023. [Online]. Available: https://ferrarispower.com/

SUNGRYUL HUH (Graduate Student Member, IEEE) received the B.S. degree in electrical engineering from Incheon National University, Incheon, South Korea, in 2018, and the M.S. degree from the CCS Graduate School of Mobility, Korea Advanced Institute of Science and Technology (KAIST), Daejeon, South Korea, in 2020, where he is currently pursuing the Ph.D. degree. His research interests include wireless power transfer system design for mobile devices and electric vehicles.

JA-IL KOO received the M.S. and Ph.D. degrees from the Electrical Engineering Department, Korea Advanced Institute of Science and Technology, Daejeon, South Korea, in 1987 and 1991, respectively. He is currently the CEO of Ferraris Inc., Las Vegas, NV, USA. He has been developed magnetic harvesting device and system for last more than ten years. He has more than ten magnetic harvesting related international patents and published more than ten.

OKHYUN JEONG (Member, IEEE) received the B.S., M.S., and Ph.D. degrees in electronic engineering from Sogang University, Seoul, South Korea, in 1982, 1985, and 1996, respectively. He has been an Associate Professor with the Department of Electronic Engineering, Sogang University, since March 2012. His research interests include power consumption and thermal management models of mobile IoT devices and wireless power charging system design for wearable robots.

SEUNGYOUNG AHN (Senior Member, IEEE) received the B.S., M.S., and Ph.D. degrees in electrical engineering from the Korea Advanced Institute of Science and Technology (KAIST), Daejeon, South Korea, in 1998, 2000, and 2005, respectively. From 2005 to 2009, he was a Senior Engineer with Samsung Electronics, Suwon, South Korea, where he was the in-charge of high-speed board design for laptop computer systems. He is currently a Professor with the CCS Graduate School of Mobility, KAIST. His current research interests include wireless power transfer system design and electromagnetic compatibility design for electric vehicles and high-performance digital systems.